

CHAPTER 4

GEOLOGY, SEISMIC RISK ANALYSIS AND EARTHQUAKE HAZARD ASSESSMENT

4.1. Surface Geology of the Damietta Harbor Area

Based on field observation and textural constituents, the studied surficial environments are generally described below.

a) River sand. The Nile River samples are moderately sorted ranging in size from fine-to medium-grained sands. These sands are mainly enriched in light and heavy minerals. Common accessory components include mica and carbonate fragments. This fluvial facies is characterized, among the other sand facies, by hosting the highest percentages of pyrite, sponge spicules and gypsum. Biogenic components, in general, and glauconite contents are the lowest compared with all the other facies.

b) Coastal dune sand. This facies is characterized by very well-sorted and very rich in fine- to medium grained laminated sands, and distinguished by the lowest proportions of carbonate fragments, and also by their abundance of heavy minerals, (Fig.4.1). The proportion of light minerals is intermediate relative to other sand facies. Mica and glauconite pellets are common, but their proportions are not diagnostic.



Fig. (4.1): photograph showing the very well-sorted and very rich in fine-medium grained sands of the coastal dune sand facies, note the mica streaks are common.

c) Accretion ridge sand. This facies is very poorly sorted varying in size from very fine to coarse sands. The most characteristic feature of this environment is its

relative enrichment in light minerals, carbonate and shell fragments, (Fig. 4.2 A & B). It is very poor in heavy minerals and mica. Glauconite and gypsum are significant components. Accretion sand ridges are normally formed by littoral currents along down slope areas of depositional sinks.

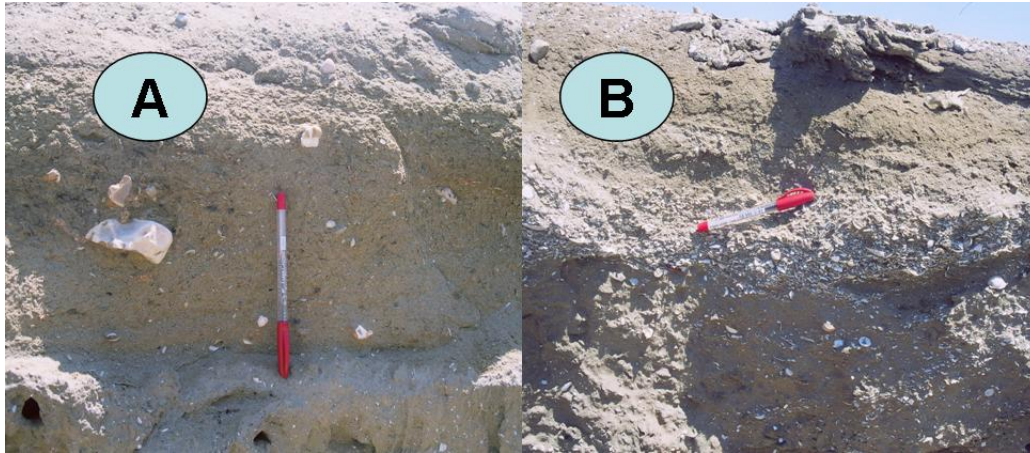


Fig. 4.2. Photograph showing the poorly sorted sand of the Accretion ridge Sand, note the shell fragments.

d) Beach sand. The beach sands are well-sorted, fine to medium-grained sands. This facies is characterized by its relative enrichment in heavy minerals, as well as by the presence of some reworked marine biogenic components, (Fig. 4.3 A&B). The light mineral content is relatively lower than that of the river or dune sands. With respect to mica proportion, it is the second largest after the nearshore facies.



Fig. (4.3) : photograph showing the beach sands, note the dark color due to the relative enrichment in heavy minerals.

e) Near shore sand. This facies is composed of poorly to moderately sorted muddy sands. Compared to the other sand facies, the near shore sand has relatively high percentages of glauconite, mica, foraminifera and plant remains, (Fig. 4.3B). The light minerals record their lowest contents, while the heavy mineral content is intermediate. Carbonate fragments, ooids and gypsum are relatively significant components.

4.2. SEISMIC RISK ANALYSIS AND EARTHQUAKE HAZARD ASSESSMENT

The extension area to the Damietta New Port lies between 31 46 15 E and 31 46 36 E and between latitudes 31 27 14 N and 31 27 38 N, it is influenced by the earthquakes occur in the Eastern Mediterranean Sea and the Fayoum-Cairo trend, Northeastern Egypt Plusiem regions. Figure (4.4) shows the location of the area of study relative to earthquake sources and source zones.

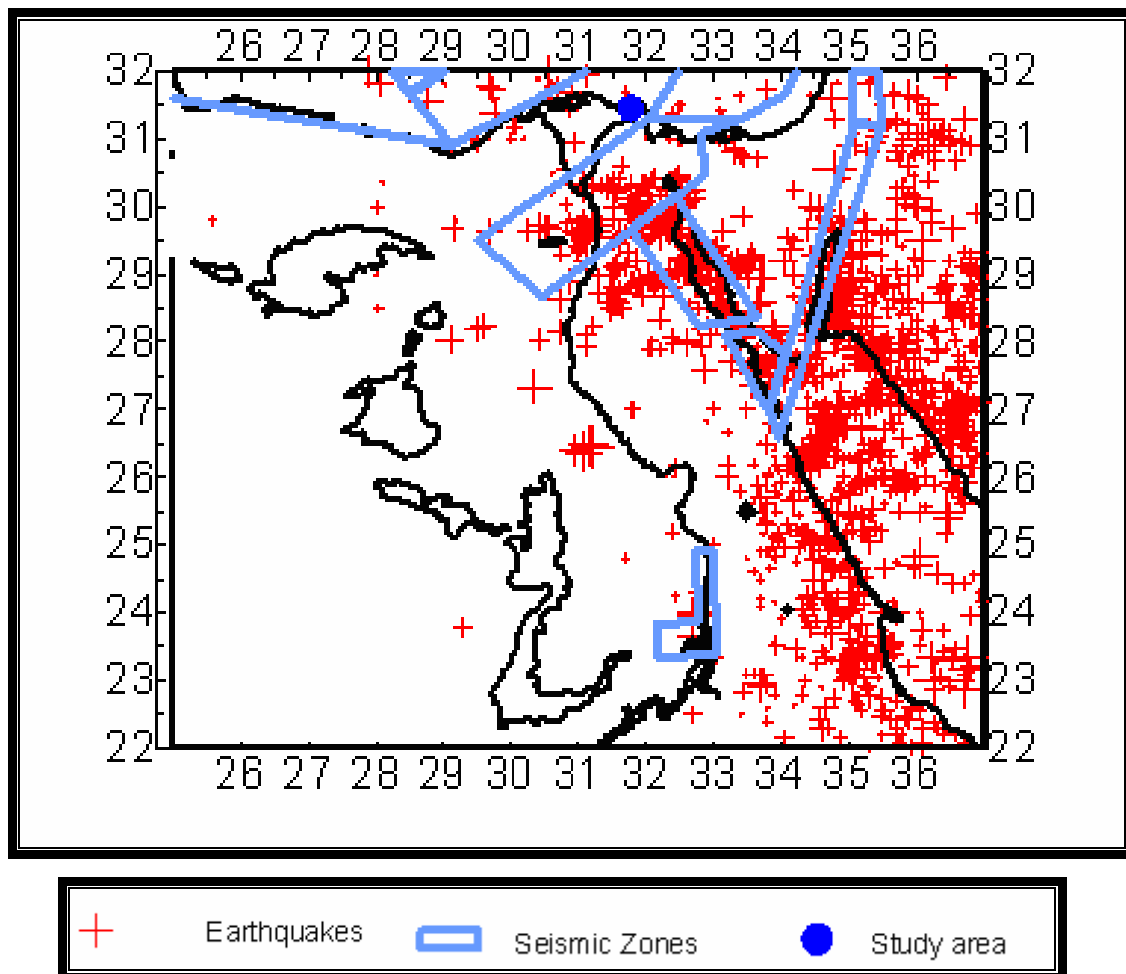


Fig. 4.4. Map showing the study area lying just outside the Cairo Fayoum and the Southeastern Mediterranean seismic source zones.

The first step in estimating the earthquake hazard at the study area is to determine most influential source areas that are capable to induce noticeable ground shaking in the area of study. These source areas could be inside or just outside the Egyptian territories as indicated in Fig. 4.4. From the said figure one can state that the

area of study occurs just on the border of two source zones; El Fayoum-Cairo-Northeastern Egypt source zone and Southeastern Mediterranean source zones.

The source zone parameters estimated from the compilation of its historical (where available) and instrumental seismicity.

4.2.1. Source Zones Inducing Earthquake Hazards to the Egyptian Land

The study included different sources that have induced or capable to induce seismic hazard to Egypt land; these are:

- Northern Gulf of Suez Zone;
- Southern Gulf of Suez Zone;
- Gulf of Aqaba;
- NW coast of Egypt;
- Dead Sea Fault zone;
- Southeastern Turkey; Southern
- Crete;
- South east and southwest Greece;
- Southeast the Mediterranean;
- Cyprus Island;
- Northeastern Libya, and
- The Red Sea

In addition to these source zones, El Fayoum-Cairo–Northeastern Egypt source zone has a special emphasis.

The earthquake catalogue used for the present study included more than 10,000 instrumentally recorded events in addition to important and well documented historical events affected the Egyptian territories. The records variably cover the period from 2200 BC up to 2003. Earthquake data was processed and dealt with using the standard techniques for verification, calibration and harmonization, so that they can be statistically treated with liable confidence.

Fig. 4.5 showed the historical earthquakes that occurred near the study area. Table 4.1 illustrates some of the historical and recent earthquakes that caused noticeable damage in areas of the Egyptian territories.

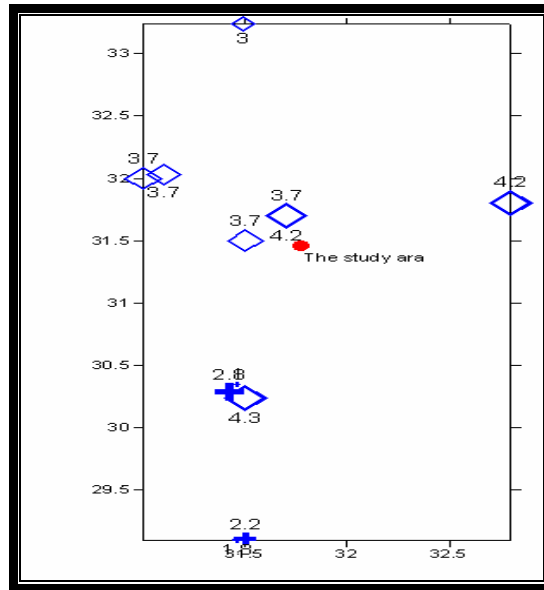


Fig. 4.5. Some of the earthquakes that occurred near the area of study.

Table 4.1 Historical and recent earthquakes, in Egypt.

Year	Area Location	Description	Magnitude /Intensity
2800 BC	Sharquia province, east Nile delta, Unknown location (1)	a severe earthquake occurred in Lower Egypt. Deep fissures and soil cracks were reported at Tell Basta, about 16 km E-SE of Zagazig.	maximum intensity VII
1/1/956	Alexandria and Cairo Unknown location (2)	Egypt was shaken by an earthquake for 3 hours; it caused great damage and many houses collapsed	Alexandria I = VIII, Cairo I = VI
8/8/1303	Offshore Mediterranean, Located outside Egypt (3)	<ul style="list-style-type: none"> The south of Cairo, perhaps in the faulted region of Mokattam and Gebel Turah, but more likely in El Fayoum. A large area of Cairo was sacrificed, several famous mosques were destroyed. Damage was also considerable in Alexandria; a large part of the town walls and the 120-m- high beacon collapsed. 	
26/6/1926	Aegean, Located outside Egypt (4)	Damage caused in Egypt was the subject of a detailed description. A zone of Intensity VI to VII was assigned to extend along the western bank of the Nile delta from Alexandria to Cairo; six houses collapsed at Alexandria	M=7.7, A zone of Intensity VI to VII was assigned to extend along the western bank of the Nile delta from Alexandria to Cairo;
12/9/1955	Mediterranean, Located outside Egypt (5)	An earthquake felt strongly in Egypt where 22 lives were lost and damage occurred in the Nile Delta between Alexandria and Cairo.	M=6.1, maximum intensity V to VI was reported in more than 15 localities The majority of the survey localities indicated intensities ranging from IV to V.

Table 4.1. Cont'ed

31/3/1969	Red Sea, Located within Egypt (6)	A Disturbances of various descriptions had been reported locally by the workers in the Shaker Lighthouse and many fishermen at the port of Hurghada. A native who lived in the region described the motion as sharp and mainly vertical in the area near the epicenter. Minor damage was reported from St. Catherine's Monastery, 110 km from the macroseismic epicenter	M=6.3 maximum intensity of IX was assigned to a small area in the islands of Shedwan, Tawaila, and Jubal (Fig. 4.4).
12/10/1992	Fayium, Egypt (7)	A relatively moderate-magnitude earthquake with epicenter about 40 km southwest of Cairo, in Dahshour, caused a great amount of damage (estimated at more than LE 500 million) and the loss of many lives.	M=5.9
22/11/1995	Gulf of Aqaba, inside Egypt	A strong earthquake with magnitude 7.1 with epicenter located in the southern part of the Gulf of Aqaba, 350 km southeast of Cairo. Most of the reported damage was concentrated in Sinai where a number of hotels were damaged leading to the loss of three lives and the injury of ten people	M= 7.1 The intensity of this event in Cairo is evaluated to be between V-VI

Sources:

- (1) Sieberg (1932 b), Woodward and Clyde Consultant, 1985
- (2) Poirier and Taher, 1980, Ambraseys, 1961
- (3) Sieberg (1932b), Woodward-Clyde Consultants, 1985
- (4) Sieberg (1932b),
- (5) Karink, 1969, Rothe, 1969
- (6) Maamoun and El Khashab (1978)
- (7) Al Ahram newspaper

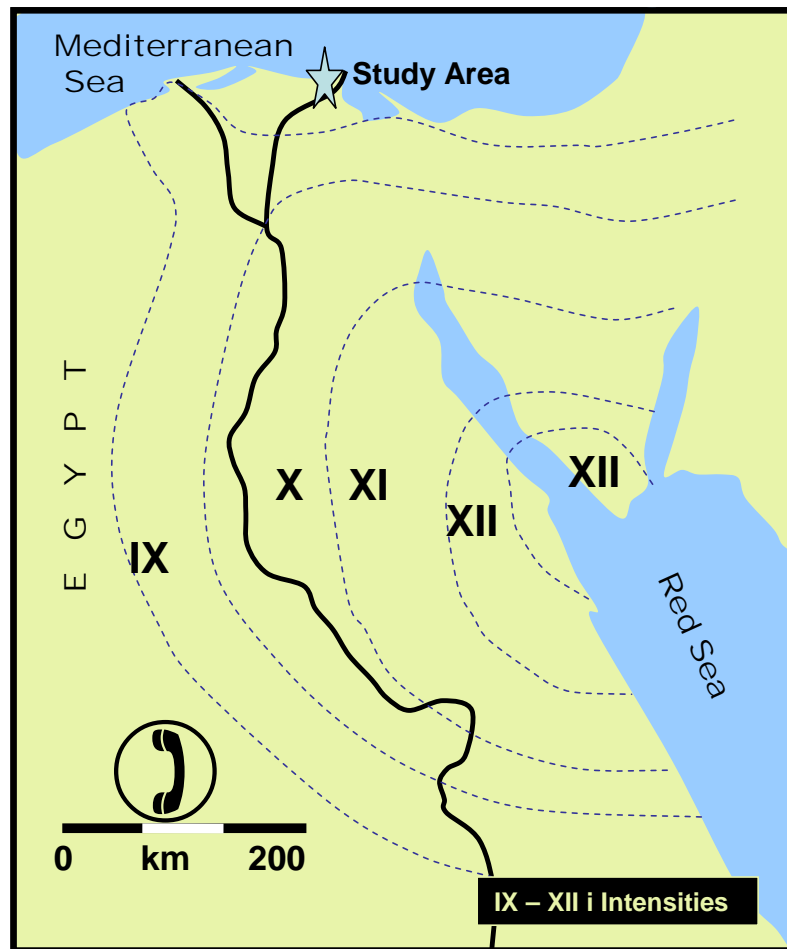


Fig. 4.6. Shedwan Earthquake (M= 6.9) Intensity Map, (Re-draw after Mamoun and Kebasy, 1990)

4.2.3. Seismic Hazard Assessment

Studies concerned with evaluating seismic hazards related to ground shaking require the prediction of strong ground motion from earthquakes that pose a potential threat to the public, either by injury or damage to property. To make such a prediction, one must know certain fundamental characteristics of these earthquakes, as they relate to the source of the seismic waves, the medium through which the waves propagate, the local geology, and the structures located at the site. If a sufficient number of strong-motion recordings from earthquakes and sites having the same or similar characteristics as those being evaluated are available, then it is straightforward to select an ensemble of these recordings for evaluating or designing structures

located at these sites for seismic loads. Estimates of strong ground motion using this approach are currently referred to as site-specific .

Seismicity Parameters

The parameter most commonly used to characterize earthquake size in strong-motion-attenuation relations is earthquake magnitude. Magnitude is the only source parameter routinely reported by seismographic networks. Other source parameters used in the past have included source dimensions, seismic moment or moment magnitude (McGuire and Hanks, 1980; Hanks and McGuire, 1981; McGuire et al., 1984).

The magnitudes of the earthquakes occurred from different source zones were used to estimate *the seismicity parameters (a & b)* as shown in table (4.2) using the Richter magnitude frequency relation ($\log N = a - bm$). These parameters are used along with attenuation information to deduce the Peak Ground Acceleration (PGA) at the site.

The following table depicts the seismicity parameters for the source areas that affect or may affect the site of interest. Attenuation formulas used are those published for US Midwest because of the scarce information available for Egypt. The Midwest US is tectonically similar to Egypt.

The seismicity parameters were convolved with the attenuation formulas using SeisRisk III program (Bender and Perkins, 1989) in order to estimate the PGA at the site for both 50 and 100 years with a probability of 0.95 of not exceeding estimated values. The 50 and 100 years are chosen as the estimated lifetime of the engineering installations. Figures (4.7 and 4.8) show the PGA at and around the site for the coming 50 and 100 years.

Table (4.2): Seismicity parameters of the source zones affecting the site

<i>Maximum possible EQ</i>	<i>b</i>	<i>a</i>	<i>Source zone</i>	<i>serial</i>
7.2	1.09	4.47	Southern Gulf of Suez	1
6.5	1.09	3.5	Northern Gulf of Suez	2
7.2	0.87	4.5	Gulf of Aqaba	3
7.0	1.00	2.54	Cairo-Fayoum- NE Egypt	4
7.3	0.96	2.2	Northern Red Sea	5

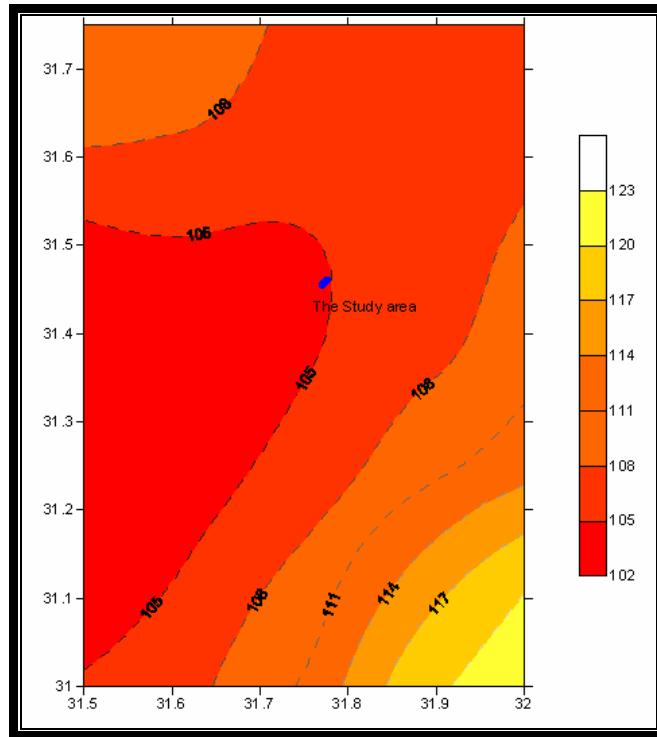


Fig. 4.7. Estimated maximum horizontal acceleration due to earthquake in 50 years to come 95 % probability of non exceedence.

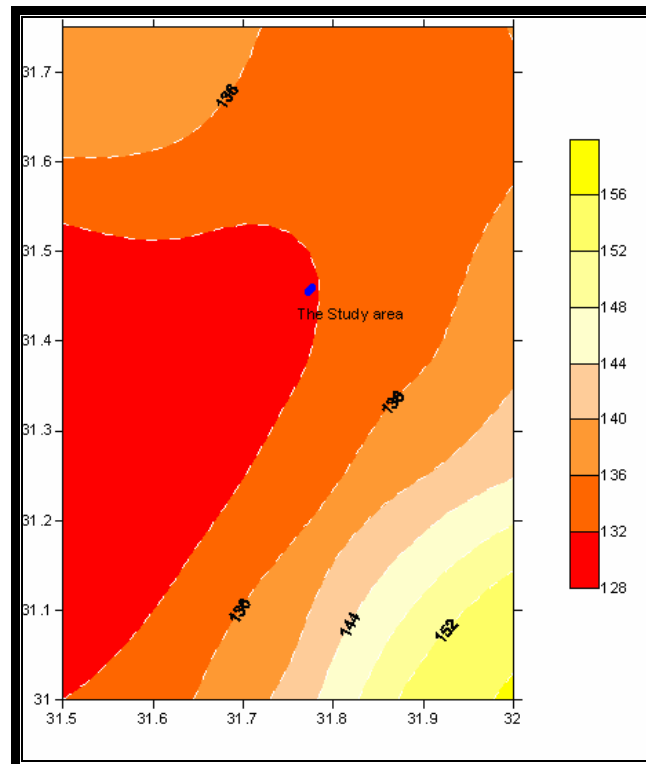


Fig. 4.8. Estimated maximum horizontal acceleration due to earthquake in 100 years to come 95 % probability of non exceedence.

As depicted in figures 4.5 & 4.6 the estimated PGA in milligals due to earthquake loads, estimated at the bedrock, during the next 50 year is about 105 milligals, while the estimated PGA during the next 100 years is about 132 milligals. These ground motion levels are calculated at 2 HZ frequency (predicted predominant frequency at the site) and are subject modification by the soils. Tthe estimated PGA levels be multiplied by 1.3 (predicted by Borchardt and Glassmoyer, 1993 as the amplification factor for loose silty sand soils) to account for the effect of the soil on the amplification of the PGA before utilized in calculating the base shear for any structure.

4.4. Downhole Seismic Velocity Measurements and Evaluation of Elastic Constants at Damietta Port

(Additional Data Acquired from Petrochemicals Co Terminal(inside the Damietta New Port)

This method is commonly used to determine compressional and shear wave velocity versus depth. These velocity data are used to help assess the seismic response and determine stratigraphy of a particular site. In a downhole seismic survey, a seismic source is placed on the surface near a downhole, and three geophones are placed at selected depths in the downhole. The raw data obtained from a downhole survey are the travel times for compressional and shear waves from the source to the geophones and the distance between the source and geophones.

Damietta Harbor is one of the areas that possess weak soil in the form of soft clays silts and as a result of water saturation also the existence of shell fragments some times. The site is divided into two main sites at which two different sets of data are acquired. One is inside Damietta Harbor (D1 and D4) and the other in northward (D2, D3 and D5). The studied area is considered flat with little or no variations in elevations. The aim of this study is to monitor the change in soil properties in terms of seismic velocities (P-Wave and S-Wave) as well as variation in ELASTIC CONSTANTS properties continuously 1-35 m depth.

Instrument Used and Testing Equipment

3-D Downhole Geophone Dhtg 50/100: A 3-D DHTG downhole geophone was used Fig. (4.9). The system consisting of (a probe, a control unit and a cable with cable reel). It is in fact characterized by a reliable clamping system, obtained through the progressive bending of a harmonic steel spring aside the probe. A powerful continuous current motor, controlled by the surface electronics, moves a piston inside the probe, controlling the bending of the spring and providing for the clamping and unclamping operations. Inside the probe there are three 10Hz geophones -oriented along the x-y-z axes - to determine the arrival time from the seismic waves of type "S" to the geophone. The main specification of the instrument used is mentioned in Table (4.3).



Fig. 4.9. 3-D downhole geophone DHTG 50/100 (Sources: www.pasigeophysics.com)

Table (4.3) Specifications of the Instrument used to record the Downhole seismic velocities.

TECHNICAL FEATURES DHTG-50 (SIS-070-000) – DHTG-100 (SIS-071-000)	
<i>Probe material</i>	Stainless steel
<i>Length cable (on cable reel with small wheels)</i>	50 / 100 m
<i>Power supply</i>	12V rechargeable internal battery (with discharge signal)
<i>Motor</i>	Electric, 12V, 10W with mechanical scaling
<i>Protection</i>	Electronic circuit with current overcharge control and protection
<i>Probe diameter</i>	40 mm
<i>Probe Length</i>	680 mm
<i>Downhole diameter (standard spring)</i>	Min.70 mm ; Max.170 mm
<i>cable reel dimensions</i>	640x300x680 mm
<i>Control unit dimensions and weight</i>	270x250x130 mm; 3kg
<i>Probe weight</i>	3.5 kg
<i>Probe weight (probe + 50m cable + reel + control unit)</i>	13 kg

Seimograph: For this testing we have used a sensitive 3-channel seismograph with Amplifier/Signal Conditioning Card, Data Acquisition Card.

Impulse Hammer: An impulse hammer is required to strike a metallic plate to induce transient vibrations. The impulse hammer used for this study was a 10 Kgm. It is capable of generating transient vibrations with frequencies as high as 2000 Hz, depending on the material at the tip of the hammer. The head of the hammer tip is 5.1 cm (2 in.) in diameter and can induce a force with a magnitude as high as 22 kN (5000 lb). Each hammer is modally tuned to eliminate multiple impacts.

The force measurement is recorded with an integral quartz force transducer mounted on the striking end of the hammer head. This quartz transducer is a piezoelectric material that develops an electrical charge proportional to applied pressure or deformation. A micro-electric amplifier circuit is incorporated into the transducer housing to improve the output signal-to-noise ratio. The sensitivity of each hammer varies slightly and was determined by the manufacturer. The magnitude of the force created by a hammer impact is calculated by dividing the measured voltage by the sensitivity. Generally speaking, the material at the hammer tip affects the hammer impulse frequency content, and the hammer mass and velocity at impact will affect both the frequency content and the energy level.

Acquisition and Interpretation Software

Advanced acquisition and interpretation softwares were used for data handling and interpretation (1999 version), both softwares were able to apply different filters and processing steps for better viewing of arrival times and excluding the final subsurface geological models and corresponding geotechnical properties.

Testing Procedure

Downhole Surveys: Five downhole surveys 3-component each (Triaxial: V_p , V_s and V_z) is recorded each one-meter, for continuous 35 m depth for all downholes. The recording was obtained for each downhole in both downhole and uphole directions for better checking to the results. Moreover for the purpose of S-wave measurements another set of data was recorded using the wooden beam and horizontal striking as discussed before. Downhole seismic measurements for downholes D1 and D4 were recorded at Damietta harbor while downholes D2, D3, and D5 was recorded northward from this site.

4.3.2. Results and Discussions

Downholes Seismic Surveys for (D2, D3 and D5): D2, D3 and D5 tend to show nearly the same properties. At downhole D2 (Fig. 4.10) the seismic velocity P-wave (interval velocity) is lower than the upper or lower interval velocities at depth range 8-23 m (15 m thick). This is most probably due to the existence of soft clays within this depth. This phenomenon is not clear from S-wave velocity recorded in the same downhole (Fig. 4.11). The main features can be determined from the elastic constants properties calculated for downhole D2 (Table.4.5). The high values obtained for Poisson's Ratio is attributed to the existence of water through the whole soil column.

At downhole D5 (Fig. 4.14) the same low velocity layer (P-wave interval velocity) is repeated again at depths 14-26 m (12 m thick) with a general tendency to become deeper than that obtained at D2. Again the elastic constants for downhole D5 suggest the existence of soft clay contents. This can be observed from the lower values obtained for *Shear Rigidity Modulus* (The yellow marked low shear rigidity modulus). Another feature, is the highly concentration of water arising from the high Poisson's ratios obtained for the whole soil column exist at D5.

At downhole D3 the obtained P-wave interval velocity is not fully representative to the soil column exists at this downhole (Fig. 4.12). This is may be because of bad well to PVC coupling or any other field problems. Although this is the case we can realize the existence of the same low velocity layer in terms of interval P-wave velocity at depth ranging between 10-28m (18 m). This can also be confirmed from the elastic constant properties obtained at Table.4.6.

Downholes Seismic Surveys for D1 and D4: Both downholes D1 and D4 (Fig. 4.10 & Fig. 4.13) show a higher interval velocities rather than D2, D3, and D5 (Fig. 4.11, 9.12 and Fig. 4.14). In downhole D1 the low velocity layer exists at depth ranging between 11-27 m (16 m) with some peaks of velocities at certain depths. These peaks can be attributed to the existence of intercalations of sands inside soft clays for example. At downhole D4 the weak soil seems to exist at depths between 10-19 m (~9m) with low interval P-wave velocity. The properties of this weak soil of Downhole D1 and D4 can be determined again from the calculated elastic constants presented at Table. (4.4) and Table. (4.7). More in situ seismic downhole surveys are needed for more accurate picture about soil variations.

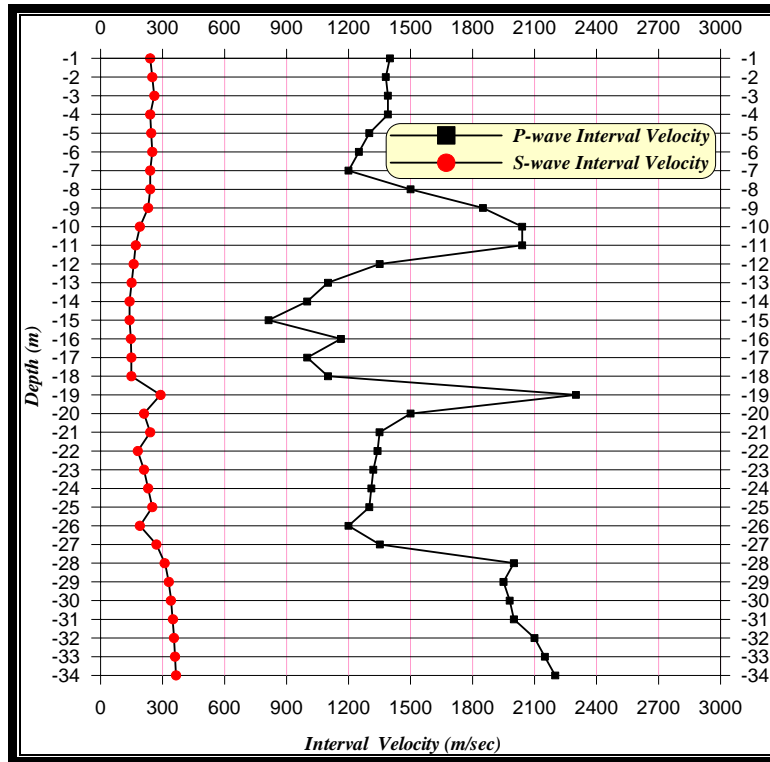


Fig. (4.10): Downhole Seismic survey for well D1

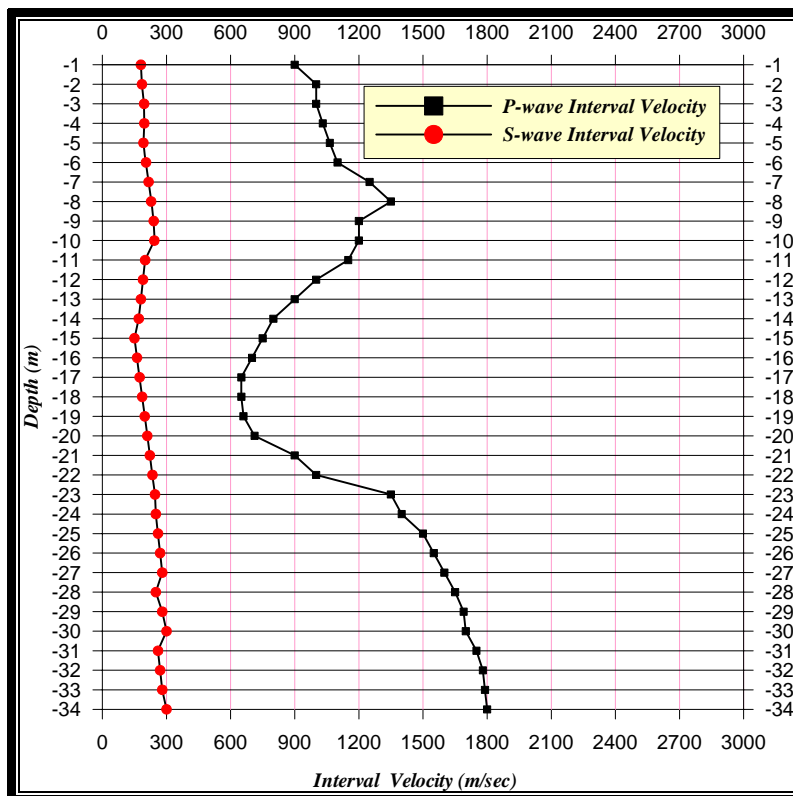


Fig. (4.11): Downhole Seismic survey for well D2

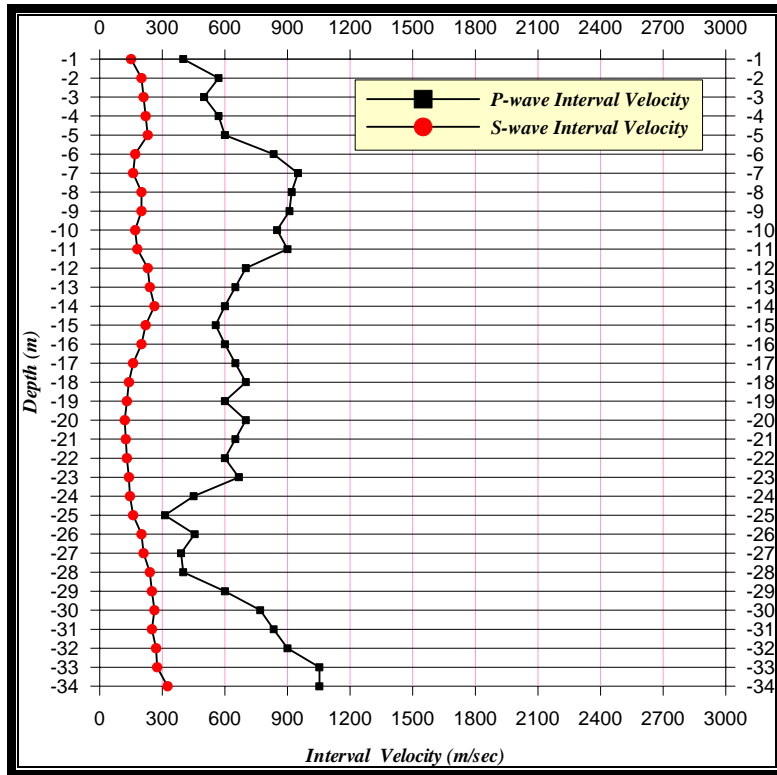


Fig. (4.12): Downhole Seismic survey for well D3

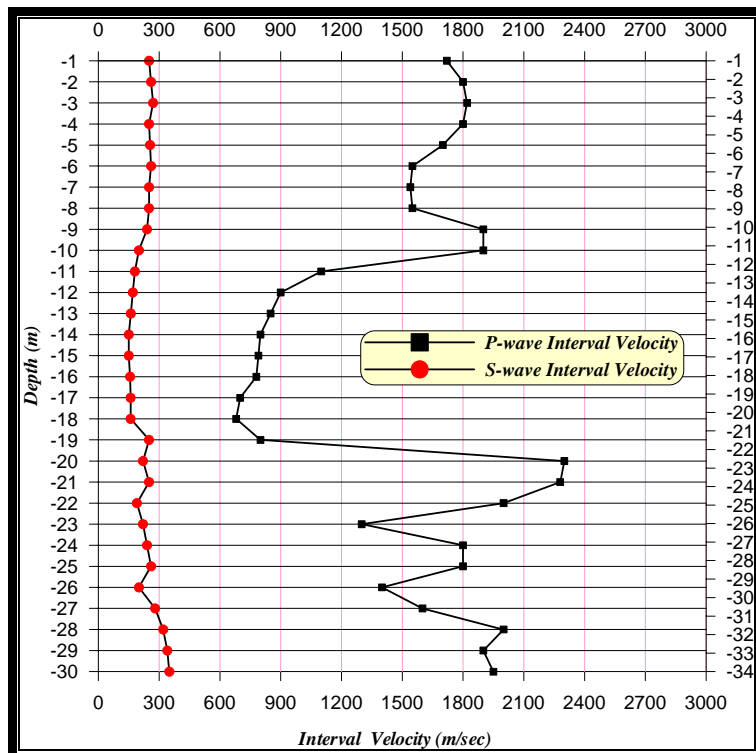


Fig. (4.13): Downhole Seismic survey for well D4

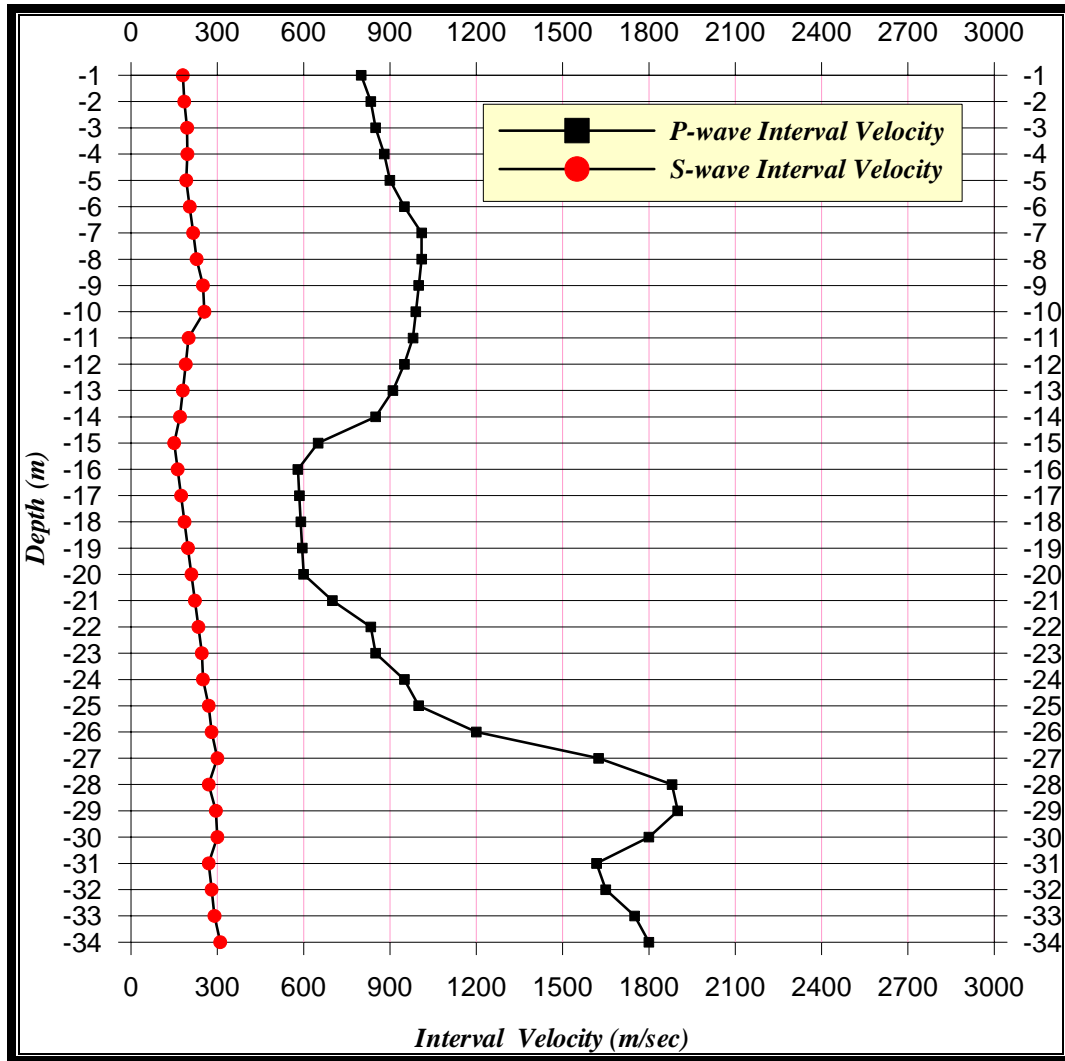


Fig. (4.14): Downhole Seismic survey for well D5

Table 4.4. Elastic Constants of Downhole-D1

<i>Depth (m)</i>	<i>S-wave (m/sec)</i>	<i>P-wave (m/sec)</i>	<i>Poisson' s ratio</i>	<i>density (kgm/m³)</i>	<i>Shear modulus (Mpa)</i>	<i>Young 's (Mpa)</i>	<i>Lame's constant (Mpa)</i>	<i>Bulk Modulus (Mpa)</i>
1	240	1400	0.48	1817	105	311	3351	3421
2	250	1380	0.48	1810	113	336	3221	3296
3	260	1390	0.48	1813	123	363	3258	3340
4	240	1390	0.48	1813	104	310	3295	3364
5	245	1300	0.48	1783	107	317	2800	2871
6	250	1250	0.48	1766	110	326	2538	2612
7	240	1200	0.48	1748	101	298	2316	2383
8	240	1500	0.49	1848	106	317	3945	4016
9	230	1850	0.49	1948	103	307	6460	6528
10	190	2040	0.50	1996	72	216	8162	8210
11	170	2040	0.50	1996	58	173	8190	8229
12	160	1351	0.49	1800	46	138	3194	3225
13	150	1100	0.49	1710	38	115	1992	2018
14	140	1000	0.49	1670	33	98	1605	1626
15	140	813	0.48	1586	31	92	986	1007
16	146	1162	0.49	1734	37	111	2271	2295
17	149	1000	0.49	1670	37	110	1596	1621
18	149	1100	0.49	1710	38	113	1993	2019
19	290	2300	0.49	2057	173	516	10533	10649
20	210	1500	0.49	1848	82	243	3995	4050
21	240	1350	0.48	1800	104	308	3073	3142
22	180	1340	0.49	1797	58	174	3110	3149
23	210	1320	0.49	1790	79	235	2961	3014
24	230	1310	0.48	1787	95	281	2877	2940
25	250	1300	0.48	1783	111	330	2791	2865
26	190	1200	0.49	1748	63	188	2391	2433
27	270	1351	0.48	1801	131	388	3026	3113
28	310	2000	0.49	1986	191	568	7562	7689
29	330	1950	0.49	1973	215	638	7074	7217
30	340	1980	0.48	1981	229	680	7308	7461
31	350	2000	0.48	1986	243	722	7457	7620
32	355	2100	0.49	2010	253	753	8359	8528
33	360	2150	0.49	2022	262	779	8824	8998
34	365	2200	0.49	2034	271	805	9302	9483

Table 4.5. Elastic Constants of Downhole-D2

<i>Depth</i> (m)	<i>S-wave</i> (m/sec)	<i>P-wave</i> (m/sec)	<i>Poisson's</i> <i>ratio</i>	<i>density</i> (kgm/m ³)	<i>Shear</i> <i>modulus</i> (Mpa)	<i>Young 's</i> (Mpa)	<i>Lame's</i> <i>constant</i> (Mpa)	<i>Bulk</i> <i>Modulus</i> (Mpa)
1	180	900	0.48	1627	53	156	1212	1247
2	185	1000	0.48	1670	57	169	1556	1594
3	195	1000	0.48	1670	64	188	1543	1585
4	196	1031	0.48	1683	65	192	1659	1703
5	192	1064	0.48	1696	63	185	1794	1836
6	204	1100	0.48	1710	71	211	1927	1975
7	216	1250	0.48	1766	82	245	2594	2649
8	228	1350	0.49	1800	94	278	3094	3156
9	240	1200	0.48	1748	101	298	2316	2383
10	243	1200	0.48	1748	103	305	2311	2379
11	200	1150	0.48	1729	69	205	2149	2195
12	190	1000	0.48	1670	60	179	1549	1590
13	180	900	0.48	1627	53	156	1212	1247
14	170	800	0.48	1579	46	135	920	950
15	150	750	0.48	1554	35	103	804	828
16	162	700	0.47	1528	40	118	668	695
17	174	650	0.46	1499	45	133	543	573
18	186	650	0.46	1499	52	151	530	564
19	198	660	0.45	1505	59	171	538	577
20	210	712	0.45	1534	68	197	642	687
21	222	900	0.47	1627	80	235	1157	1211
22	234	1000	0.47	1670	91	269	1487	1548
23	246	1350	0.48	1800	109	323	3063	3135
24	250	1400	0.48	1817	114	337	3333	3409
25	260	1500	0.48	1848	125	371	3908	3992
26	270	1550	0.48	1863	136	403	4205	4296
27	280	1600	0.48	1878	147	437	4514	4612
28	250	1650	0.49	1893	118	352	4916	4995
29	280	1690	0.49	1904	149	444	5140	5239
30	300	1700	0.48	1907	172	509	5168	5282
31	260	1750	0.49	1921	130	387	5623	5709
32	270	1780	0.49	1929	141	419	5830	5924
33	280	1790	0.49	1932	151	451	5886	5987
34	300	1800	0.49	1934	174	517	5919	6035

Table 4.5. Elastic Constants of Downhole –D3

<i>Depth</i> (m)	<i>S-wave</i> (m/sec)	<i>P-wave</i> (m/sec)	<i>Poisson's</i> <i>ratio</i>	<i>density</i> (kgm/m ³)	<i>Shear</i> <i>modulus</i> (Mpa)	<i>Young 's</i> (Mpa)	<i>Lame's</i> <i>constant</i> (Mpa)	<i>Bulk</i> <i>Modulus</i> (Mpa)
<i>1</i>	150	400	0.42	1328	30	85	153	173
<i>2</i>	200	570	0.43	1451	58	166	355	394
<i>3</i>	210	500	0.39	1404	62	173	227	269
<i>4</i>	220	570	0.41	1451	70	198	331	378
<i>5</i>	230	600	0.41	1470	78	220	374	425
<i>6</i>	170	833	0.48	1596	46	136	1016	1047
<i>7</i>	160	950	0.49	1649	42	125	1404	1432
<i>8</i>	200	920	0.48	1636	65	193	1253	1297
<i>9</i>	200	909	0.47	1631	65	192	1217	1261
<i>10</i>	170	850	0.48	1604	46	137	1066	1097
<i>11</i>	180	900	0.48	1627	53	156	1212	1247
<i>12</i>	230	700	0.44	1528	81	233	587	641
<i>13</i>	240	650	0.42	1499	86	245	461	518
<i>14</i>	262	600	0.38	1470	101	279	327	395
<i>15</i>	220	555	0.41	1442	70	196	305	352
<i>16</i>	200	600	0.44	1470	59	169	412	451
<i>17</i>	160	650	0.47	1499	38	113	557	582
<i>18</i>	140	700	0.48	1528	30	89	689	709
<i>19</i>	130	600	0.48	1470	25	73	479	496
<i>20</i>	120	700	0.48	1528	22	65	704	719
<i>21</i>	125	650	0.48	1499	23	69	587	602
<i>22</i>	130	600	0.48	1470	25	73	479	496
<i>23</i>	140	666	0.48	1509	30	87	612	631
<i>24</i>	145	450	0.44	1368	29	83	219	239
<i>25</i>	160	312	0.32	1249	32	85	58	79
<i>26</i>	200	454	0.38	1371	55	151	174	210
<i>27</i>	210	390	0.30	1320	58	151	84	123
<i>28</i>	240	400	0.22	1328	76	186	59	110
<i>29</i>	250	600	0.39	1470	92	256	345	407
<i>30</i>	262	769	0.43	1564	107	308	711	782
<i>31</i>	250	833	0.45	1596	100	289	909	975
<i>32</i>	270	900	0.45	1627	119	344	1080	1159
<i>33</i>	275	1052	0.46	1692	128	374	1618	1704
<i>34</i>	325	1052	0.45	1692	179	517	1517	1636

Table 4.6. Elastic Constants of Downhole -D4

<i>Depth</i> <i>(m)</i>	<i>S-wave</i> <i>(m/sec)</i>	<i>P-wave</i> <i>(m/sec)</i>	<i>Poisson's</i> <i>ratio</i>	<i>density</i> <i>(kgm/m³)</i>	<i>Shear</i> <i>modulus</i> <i>(Mpa)</i>	<i>Young's</i> <i>(Mpa)</i>	<i>Lame's</i> <i>constant</i> <i>(Mpa)</i>	<i>Bulk</i> <i>Modulus</i> <i>(Mpa)</i>
1	250	1720	0.49	1912	120	356	5419	5499
2	260	1800	0.49	1934	131	389	6006	6093
3	270	1820	0.49	1940	141	421	6142	6237
4	250	1800	0.49	1934	121	360	6025	6106
5	255	1700	0.49	1907	124	369	5263	5346
6	260	1550	0.49	1863	126	374	4225	4309
7	250	1540	0.49	1860	116	346	4179	4257
8	250	1550	0.49	1863	116	346	4244	4321
9	240	1900	0.49	1961	113	337	6852	6927
10	200	1900	0.49	1961	78	234	6921	6973
11	180	1100	0.49	1710	55	165	1959	1996
12	170	900	0.48	1627	47	139	1224	1255
13	160	850	0.48	1604	41	122	1076	1104
14	150	800	0.48	1579	36	105	940	963
15	150	790	0.48	1574	35	105	912	935
16	156	780	0.48	1569	38	113	878	904
17	159	700	0.47	1528	39	114	671	697
18	159	680	0.47	1517	38	113	625	650
19	250	800	0.45	1579	99	285	813	879
20	220	2300	0.50	2057	100	298	10680	10747
21	250	2280	0.49	2052	128	383	10411	10497
22	190	2000	0.50	1986	72	214	7801	7848
23	220	1300	0.49	1783	86	256	2841	2899
24	240	1800	0.49	1934	111	332	6044	6119
25	260	1800	0.49	1934	131	389	6006	6093
26	200	1400	0.49	1817	73	216	3415	3464
27	280	1600	0.48	1878	147	437	4514	4612
28	320	2000	0.49	1986	203	605	7537	7673
29	340	1900	0.48	1961	227	672	6625	6776
30	350	1950	0.48	1973	242	717	7021	7182